Final Report for NASA project NAS8-99070
Microcosm, Inc.
Prepared by Dr. Henryk Szmacinski , PI

Our project on "Cellular Oxygen and Nutrient Sensing in Microgravity Using Time-Resolved Fluorescence Microscopy" led us to the development of advanced tools to monitor cellular events. During the duration of the project from May 1999 to July 2003, we have developed procedures and methods for the simultaneous imaging of intra- and extra-cellular oxygen and pH with minimal calibration procedures. There are two major advances to report: (1) Development of microscope hardware and software and (2) Development of oxygen and pH sensing chemistry and identification of probes that are compatible with lifetime methodology and technology and applicable to cellular research.

In addition to the data provided here, we also refer you to the information provided in our previously submitted annual reports dated July 31, 2000, July 31 2001 and July 31, 2002. The project has been directed by Dr. Henryk Malak (PI) from May 1999 to July 31, 2001 and continued by Dr. Henryk Szmacinski (PI) from January 1, 2001 to July 31, 2003.

1. **Time-Resolved Fluorescence Microscopy (TRFM) and Fluorescence Lifetime Imaging Microscopy (FLIM). (Task 1 – Prepare the Necessary Equipment and Data Bases, Task 2 – Prove that Miniature Hardware Works)**

Both time-resolved technologies TRFM and FLIM are not commonly used for cellular applications. This is because they require more complex instrumentation and knowledge of sensing materials that provide full benefits of lifetime-based sensing and imaging. At Microcosm we have full capabilities to develop these technologies. We have chosen a frequency-domain technique where excitation sources can utilize light-emitting diodes (LEDs). LED based excitation is of particular interest to NASA because LED instrumentation has low power consumption, requires no maintenance, can work for very long time (up to 10,000 hours), and allows for the miniaturization of instruments.

We have assembled miniaturized LEDs and tested their performances for time-resolved fluorescence. Modulation frequencies up to 20 MHz were used for testing of standard fluorophores with a short lifetime of several nanoseconds (Rhodamine B, Fluorescein) as well as a long lifetime of several hundred nanoseconds (ruthenium complexes). Also, we have found that for higher excitation demands, multiple LED's can be assembled and driven by simple electronics- bias tees, where both DC current and RF modulation signals are applied. It has been shown that modulation frequencies up to 300 MHz can be used with LED's [1].

Initially, we performed testing of our assembled LEDs' excitation and a miniaturized microscope. LEDs were combined with an epifluorescence cube and directly connected to the microscope objective. The detection system consisted of photomultiplier and customized frequency-domain fluorometer from ISS (Urbana- Champaign, Illinois). Such design allowed for a sample consisting of liquid solutions or cell suspensions and provided data on the average lifetime over the total illuminated area. Experiments on photobleaching and dye-cell interactions were performed on insect cells Sf21 that contained green fluorescent proteins (GFP). It was demonstrated that ruthenium complexes do not photobleach compared to the GFP that beached very fast. Part of these experiments were presented on conference in collaboration with NASA scientists [2].

After proof of concept that our miniature hardware worked we decided to develop a 2D TRFM (that we call FLIM) that allows for two-dimensional lifetime images of microscopic specimens. The detection system using a photomultiplier (PMT) and standard frequency-domain fluorometer was

replaced with modulated image intensifier and CCD camera, thus allowing us to transform the TRFM into FLIM instrumentation. The schematic diagram of TRFM and FLIM configurations are shown in Figure 1.
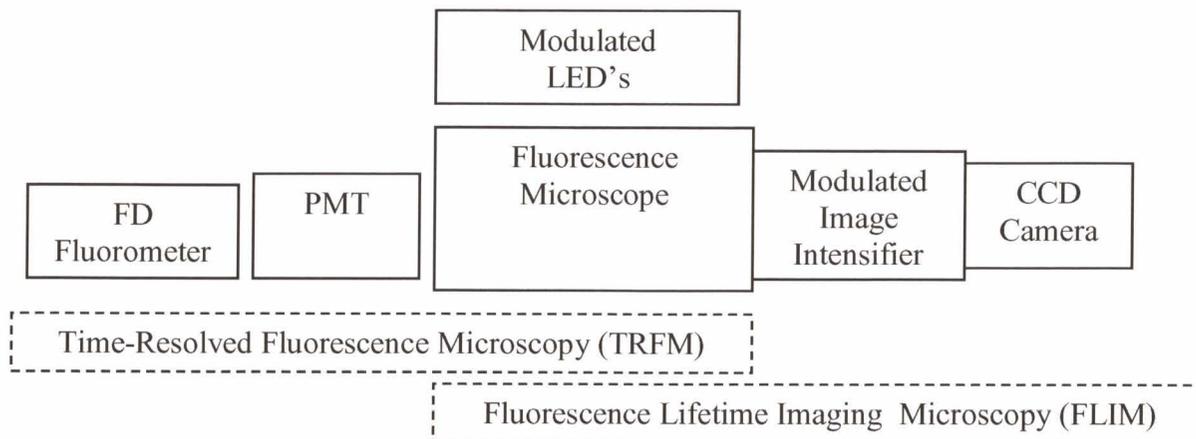
Figure 1. Schematic diagram of the TRFM and FLIM instrumentation.

Table 1. Specifications for TRFM and FLIM instrumentation

Instrument component	Description
Fluorescence Microscope	Standard wide field fluorescence microscope, e.g. Zeiss Axiovert 135. Miniaturized microscope may consists of miniaturized stage with only objective and epifluorescence cube.
Modulated miniaturized excitation source	Light emitting diodes (LED's), driven with bias tee with DC current and RF signal for modulation. DC power supply: Precision current source Model LDX-3412 from ILX Lightwave, Bozeman, MT. Bias Tee Model 5580 from Picosecond Pulse Labs, Boulder, CO. LED's: Available from Nichia: 373 nm UV (NSHU590E), 458 nm Blue (NSPB500), 530 nm Green (NSPG500), all from Nichia. Possible use of Laser Diodes with the same modulation electronics.
FD Fluorometer	Available from ISS Urbana-Champagne, Illinois. Operate up to 1 GHz with portable computer. Can be customized for smaller size.
PMT	Hamamatsu R928 is the most practical for fluorescence spectroscopy. It is available from ISS with housing and electronics for frequency-domain detection. Other PMT's can be considered for specific applications.
Modulated Image Intensifier	Hamamatsu High-Frequency-Modulated Image Intensifier Unit C5825. This is the only commercially available unit. Modulation frequency from 300 kHz to 300 MHz. We have found that unit works at lwer modulation frequencies, from 150 kHz, which is more useful for oxygen imaging.
CCD Camera	Hamamatsu Fast Scan Multi Format Cooled CCD Camera C4880-80 has been used under project. Other cooled cameras with high dynamic range (12-14 bit) can be considered.
Frequency synthesizer	PTS 310 from Programmed test Sources, Inc. PTS 310 provides the ability for computer controlled frequency, output level and phase rotation from 0-360 deg in 0.225 deg steps. Computer controlled RF signal is applied to image intensified allowing for automated phase sensitivity image acquisition.
FD software	ISS provides the software for data acquisition and data processing.
FLIM software	Microcosm developed acquisition and image processing software.

This FLIM instrument in our opinion, and as was also recognized by our NASA Program Manager, provides full benefits for NASA's cellular research. The importance of time-resolved fluorescence for imaging can be understood from the fact that unlike intensity, the fluorescence lifetime is largely

independent of the probe concentration, photobleaching, and light path. All these parameters are extremely difficult to control during microscopic cellular experiments.

We have developed software for FLIM data acquisition and image processing. Our FLIM instrument has been used for oxygen and pH sensor development for intra- and extra-cellular measurements.

1.1 Principles of FD FLIM

FLIM measurements involve taking a stack of fluorescence intensity images with a sinusoidally modulated excitation source and a detection source with a relative-phase-locked sinusoidally modulated gain at different phase (temporal) offsets in the relative phase.

$$I(r,\theta_D) = I_0(r)\{1 + 0.5 m_D m(r) \cos(\theta(r) - \theta_D)\} \qquad (1)$$

Here r is the position in the image, θ_D is the detector phase angle relative to the excitation phase angle (e.g., the vertical coordinate of the image stack), m_D is the modulation amplitude of the detector, $m(r)$ the modulation amplitude of the emission, and $\theta(r)$ the phase of the emission.

The general desire is to display the three critical components of this function graphically, as false color images describing the aggregate value of the image stack in a 2D pixel space. A vector of intensities I(r) is derived from the stack at each value of r, and fit as a linear combination of trigonometric functions

$$I(r,\theta_D) = a_0(r) + a_1(r)\cos(\theta_D) + b_1(r)\sin(\theta_D) \qquad (2)$$

The apparent fluorescent phase $\theta_A(r)$, apparent modulated amplitude $m_A(r)$, and apparent dc amplitude $D_c(r)$ are then found from

$$\theta_A(r) = -\tan^{-1}[a_1(r)/b_1(r)]$$
$$m_A(r) = [a_1^2(r) + b_1^2(r)]^{1/2}/a_0(r) \qquad (3)$$
$$D(r) = a_0(r)$$

It is these three quantities that must be computed and displayed in the FLIM software: phase angle, modulation and intensity at each pixel of the image.

In addition our FLIM software allows one to select a region of interest and calculate the average of these three values without processing the whole 2D image. This feature is valuable if one has a number of different areas with different probes.

More detailed theory of the phase and modulation FLIM can be found in the representative publications [3-4].

1.2 Procedure for FLIM data acquisition

A series of phase-sensitive images are acquired at various phase shifts of RF signal applied to the gain of the image intensifier (Figure 2). Intensity variation (cosine) at each pixel is related to the fluorescence lifetime. The stack of images is then processed to determine the phase angle and modulation factor for each pixel. This is performed on very high volume of data 262,144 pixels (512x512 image size) and 5-18 phase sensitive images (depends on phase shift increment).
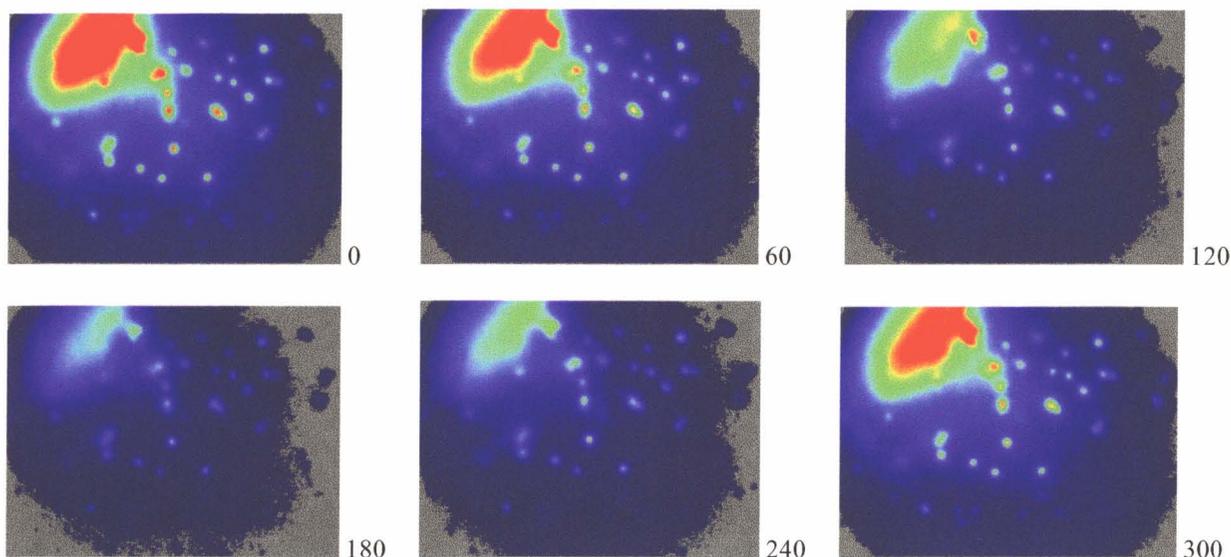
Figure 2. Phase sensitive intensity images display variation in intensity according an Equation (1). Apparently phase shift of RF signal of 0 deg is in phase with a fluorescence (high intensity) and that at 180 deg , close to out of phase (low intensity). Several phase sensitive images provide data for a calculation at each pixel of the sample image. In this case, FLIM data for three spatially various environments are acquired simultaneously: oxygen microsensor (brightest large area), yeast cells (small round areas), and culture medium (intermediate area).

1.3 Procedure for FLIM data processing

Our FLIM software allows one to select the region of interest and calcule the average phase angle and modulation, which is similar to the principle of TRFM where average lifetime is determined from the whole illuminated area. In addition, our FLIM software allows for the selection of many regions of interest (up to 20) with any size, and display intensity and lifetime information. This is illustrated in Figure 3 where three regions of interest were selected. This software feature allows one to verify the quality of data and also allows for quick analysis of multiple independent sites (e.g. microsensor area, cells, and culture medium) without time consuming processing of the entire image area. Processing of each pixel results in FLIM images of intensity, phase and modulation as shown in Figure 4.

Further, by applying known calibration curve phase and modulation, images can be converted into a chemical image. Phase calibration curves for oxygen imaging are shown in Figure 5. Oxygen probe $Ru(dppS)_3$ displays different oxygen sensitivity in culture medium and inside cells. Also oxygen microsensor (solid-state) displays its own calibration curve. In this case three converting procedures need to be performed on the phase image to determine the oxygen concentration of each area.

We have found that oxygen equilibrium for cells needs a substantially longer time than that for a microsensor and probe in culture medium (Figure 5).
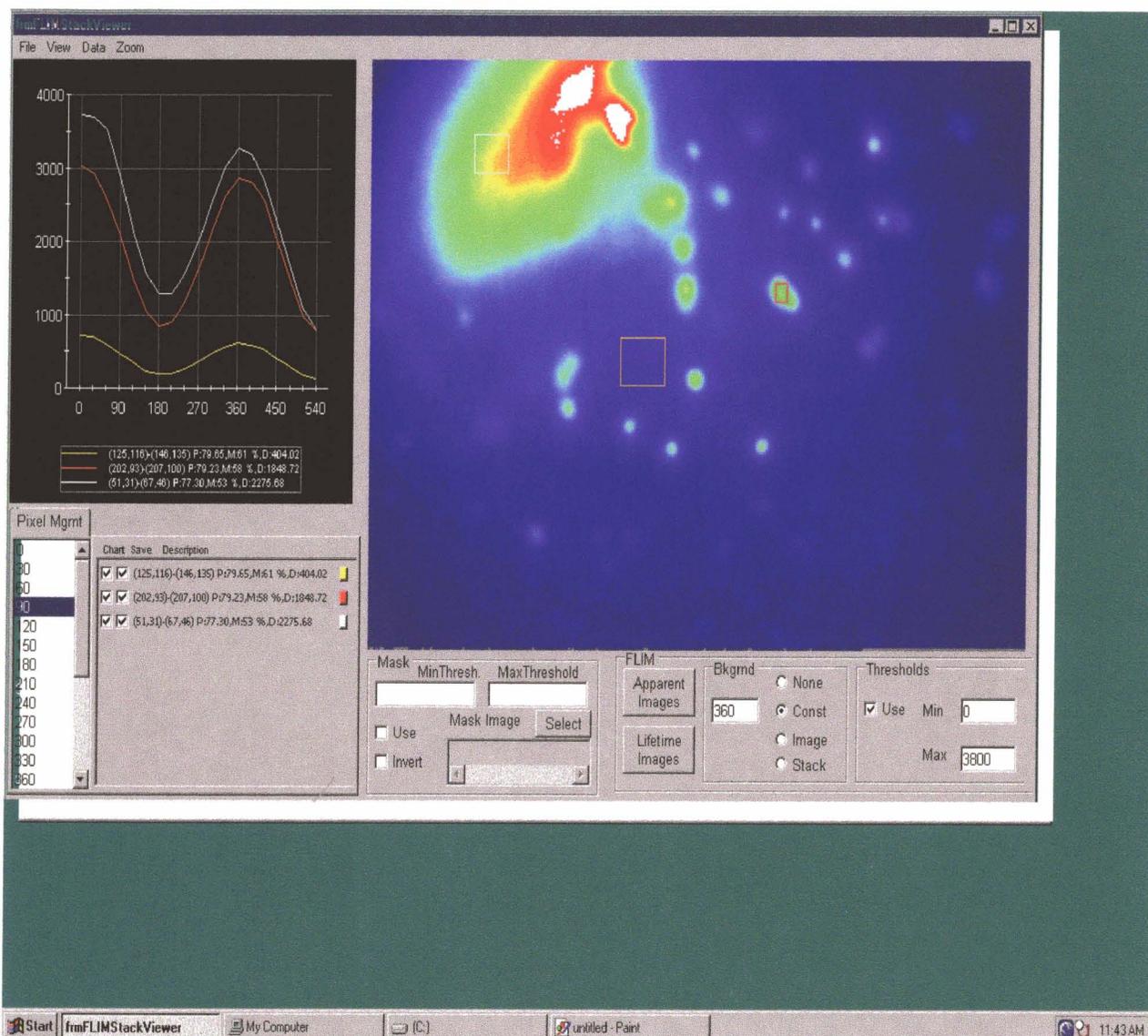
Figure 3. Procedure for FLIM data image processing. Displayed phase sensitive image is at phase shift of 90 deg. Average intensity variation (cosine) of three selected areas, oxygen microsensor (large bright patch), culture medium (blue darker area), and yeast cells (small round shape patches) are displayed on left black panel with information on phase, modulation, and intensity values. Apparent Images button initiates image processing base pixel by pixel or binned images that results in three images: phase, modulation and intensity. Further processing (Lifetime Images Button) transforms phase and modulation images into a lifetime images. Lifetime Image button can be modified to Chemical Image if the calibration curve for the used sensor is known. Mask feature allows display regions with defined thresholds of selected image.

| Intensity Image | Phase Image | Modulation Image |
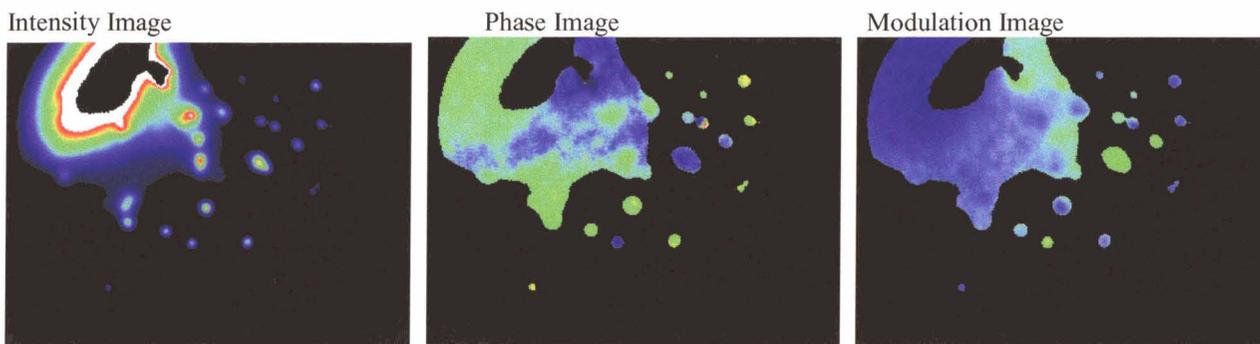
Figure 4. Three resulting images after FLIM software analysis, intensity image, phase image and modulation image. Phase and modulation images are displayed using intensity image as masking image. Here is evidence that lifetime–based sensing/imaging is independent of fluorescence intensity. While intensity of cells varies across them, phase and modulation are uniform and related to the oxygen concentration not to the probe distribution. It should be noted that lower values on phase image correspond to higher values on modulation image. Close investigation of phase and modulation images reveal that two cell populations are visible, one with lower phase angle (higher oxygen concentration, phase image-blue, modulation image-green) and second with higher phase angle (lower oxygen concentration, phase image-green, modulation image-blue.
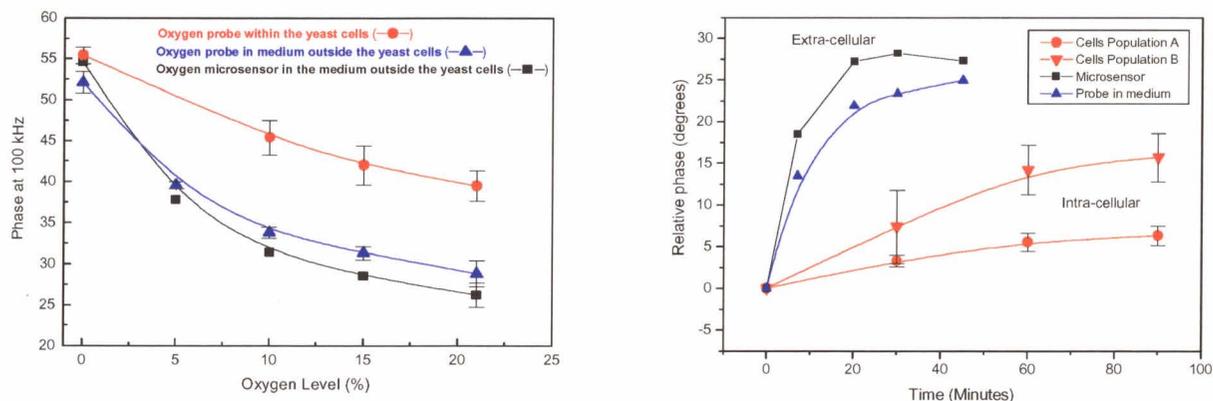
Figure 5. Left: Calibration curves for three environments. Oxygen response of microsensor and oxygen probe in culture medium is similar. An oxygen response of probe in the yeast cells is different.

2. Fluorescence sensors for oxygen and nutrient sensing (Task 3 – Select and optimize sensors for oxygen and nutrient sensing).

2.1 Oxygen sensor development

We have developed several new ruthenium complexes as potential oxygen probes. The synthesized formulations include $Ru(acp)_3$ where acp: 5-(3-amidocumarin)-1,10-phenanthroline, $Ru(eacp)_3$ where eacp: 5-(N-ethyl-3-amidocumarin)-1,10-phenanthroline. The synthesis and characterization of these oxygen probes were performed mostly under NIH grant support and less from NAS8-99070, but fortunately there was some overlap between these two programs. These new oxygen probes displayed better spectral properties in organic solvents compared to commercially available $Ru(phn)_3$ that make them potential probes for polymer-based oxygen sensors. A manuscript on synthesis and spectral properties of the above oxygen probes has been submitted [5].

We have found that ruthenium complex with sulfonate group, $Ru(dppS)_3$, dppS: 1,4-diphenyl 1,10-phenanthroline sulfonate provides excellent conditions for oxygen sensing in aqueous culture

media and is uptaken by cells. This oxygen probe displays excellent oxygen sensitivity, high quantum yield, and very good water solubility. Ru(dppS)₃ has been obtained from Center for Fluorescence Spectroscopy, University of Maryland. The chemical procedure for synthesis is described in detail elsewhere [6]. Table 2 summarizes spectroscopic properties of oxygen probes evaluated under the project.

Table 2. Spectroscopic properties of oxygen probes compatible with FLIM technology

Oxygen probe/solution	Exc/Em (nm)	Lifetime			Comments
		N_2 (ns)	Air (ns)	Ratio	
Ru(phn)₃ /acetonitrile	447/595	440	85	5.2-fold 2.0	Available from Aldrich
Ru(acp)₃/acetonitrile	453/597	1280	142	9.0 1.4	Synthesized under project, submitted for publication, Ref. 5
Ru(eacp)₃/acetonitrile	450/601	630	158	4.0 1.9	
Ru(dppS)₃ /water	440-470/610	3850	863	4.5	From CFS UMAB, synthesis described in Ref. 6 High content of proteins will result in decreased oxygen sensitivity.
Silicone-based oxygen microsensor (Ru(dpp)₃)	452/605	5331	691	7.7	Embedded dye into a pre-fabricated silicone substrate
		4857	611	7.9	Homogeneously mixed dye with liquid silicone and polymerized.
		5056	2661	1.9	Embedded dye from methanol solution into a polystyrene beads

Oxygen microsensors using silicone solid-state support have been also fabricated and evaluated to the submicometer size (thickness). We demonstrated that these microsensors provide excellent extracellular oxygen sensing capabilities regardless of the chemical composition of the sensing medium. Two methods can be used to fabricate silicone based oxygen microsensors: (i) entrapping a probe into a fabricated microstructure from dichloromethane solution (soaking method); or (ii) fabricating a liquid mixture of silicone and probe and polymerization of desired size of the microsensors. Both methods resulted in very good oxygen sensor performances (Figure 6).
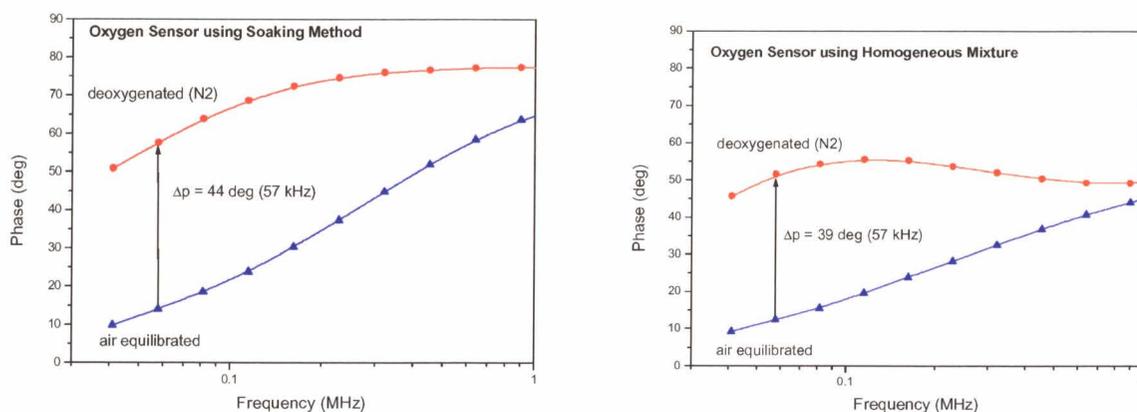
Figure 6. Silicone-based oxygen sensors display high oxygen sensitivity as demonstrated with changes in the phase angle in the oxygen concentration range from 0 (nitrogen equilibrated) to 21 % (air equilibrated). Both fabricaton methods (soaking method and homogeneous) allow for wide range of modulation frequencies to be used for oxygen sensing (from approximately 20 kHz to 400 kHz which allows to match modulation frequencies for pH FRET-based sensors (1rom 100 kHz to 500 kHz)

2.2 pH sensor development

Development of pH sensors using metal-ligand complexes is a challenging chemical task. First, the pH range that can be measured by known ruthenium complexes are low with pKa about 4 and less. We have identified commercially available (Fluka) ruthenium complexes that display pH sensitivities, Ru(bpy)$_2$(dcbpy) and Ru(bpy)$_2$(mcbpy). We have characterized them as potential pH probes for low pH range measurements. They display sufficient pH sensitive lifetimes and relatively low pKa's (Table 3). For higher pH ranges, we have synthesized a pH probe Ru(phn)(DEAM-bpy) where DEAM-bpy: 4,4'-bis(diethylamino-methyl)-2,2'-bipyridine). This probe displays better pH sensitive properties than recently published ruthenium pH probe for neutral pH range [8]. The pH probe synthesis and its use has been filed for patent application [9]. Our synthesized pH probe displayed desired properties: pKa ~ 7.2, pH sensitive emission spectral shift, and most important pH sensitive lifetime.

Ruthenium complexes have not been used for cellular applications, mainly because there was no availability of such probes. We have incubated cells with pH ruthenium probes but have not obtained pH sensitive responses. Also, the signal from these cells was very weak. Our attempts involved utilizing our model yeast cells. To determine their usefulness for cell research requires expertise from physiology area. In Table 3 are summarized spectroscopic properties of pH probes and FRET-based pH sensors investigated under project. There are also references for additional lifetime pH sensitive probes commercially available.

We developed pH sensors based on energy transfer that are particularly useful for extra-cellular applications. These include a ruthenium complex that is pH insensitive and a pH indicator with the desired pH sensitivity range. We demonstrated that pH microsensors could be fabricated for pH ranges from pH 3 to 9 with very high pH sensitivities. Figure 7 shows the superior sensitivity of a FRET-based pH sensor versus intrinsic pH ruthenium-based probes. The second graph in Figure 7 shows that FRET-based sensors perform well in various aqueous media.

Table 3. Spectroscopic properties of pH probes compatible with FLIM technology

pH probe	Exc/Em (nm)	Lifetime		pKa	Comments
		Acid (ns)	Base (ns)		
Ru(bpy)$_2$(dcbpy)	450/610	242	468	3.95	Available from Fluka
Ru((bpy)$_2$(mcbpy)	450/610	116	472	4.40	Available from Fluka
Ru(phn)$_2$(DEAM-bpy)	450/623-645	361	609	7.2	Synthesized under project, patent application, Ref. 8
Ru(bpy)$_2$(deabpy)		269	475	7.5	Described in proposal, Ref. 7
FRET-based pH sensors	455/615	Variable ~ 100 ns	Variable ~ 1200 ns	Variable 3 – 8	Emission of Ru(dppS)$_3$ pH range dependent on pKa of the pH indicator, see below for CPR and TBPSP based sensors.
Oregon Green 488	488/530	2.24	3.86	3.8	Available from Molecular Probes, cell permeable form Other probes available, see Ref. 9-11
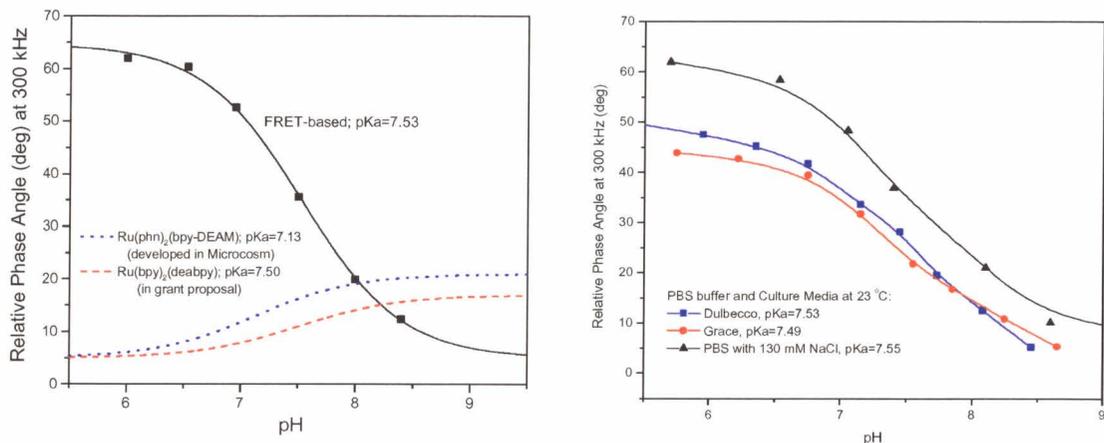
Figure 7. Left: FRET-based pH sensor display superior pH sensitivity over the ruthenium intrinsic pH probes. Right: Calibration curves for pH sensor are culture medium dependent.

We have discovered that FRET-based solid-state pH sensors display shifts in pH sensitivity dependent on the sensor's thickness. We have fabricated solid state pH sensors using two pH indicators, chlorophenyl red (CPR) and tetrabromophenylsulfonephthalein for low and high ph range , respectively. We also found that calibration curve for microsensors (thickness ~ 1 um) and macrosensors (100 um) may substantially differ. The pH sensitivities and effect of thickness on the calibration curve are shown in Figure 8.
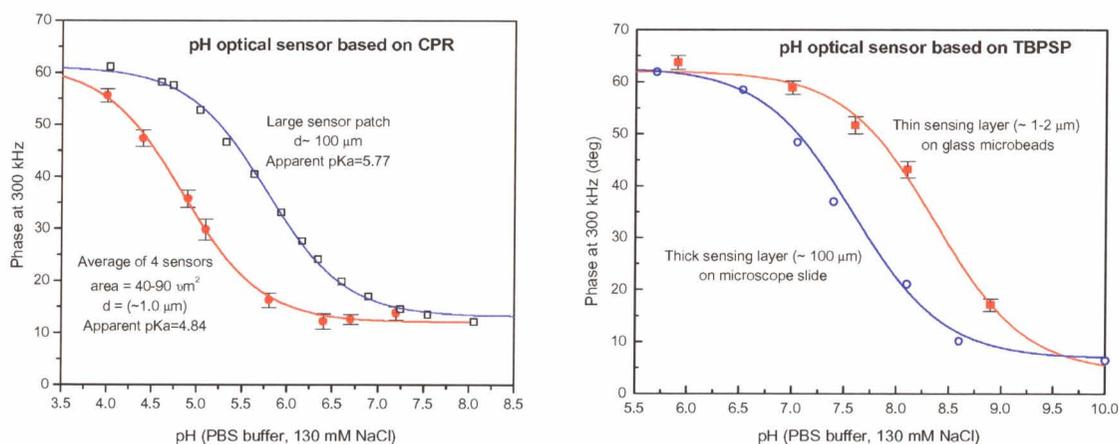
Figure 8. pH response of microsensors are dependent on the sensor thickness. This may allow of multiple pH sensors spatially distributed with various sizes for FLIM data to cover a larger pH range. For example using CPR one may measure pH from pH 3 to pH 7, i.e. four pH units instead of approximately 2 pH units with one sensor size.

Our efforts to employ ruthenium complexes for pH cellular sensing were designed to have a simplified instrumental setup with the same electro-optical design for oxygen and pH sensing. We intended to use single set of filters and modulation frequencies that matched the oxygen and pH sensing requirements. If the difficulties encountered with ruthenium based probes loading into cells can be solved, it will open an opportunity for simpler operation of FLIM instrumentation (i.e. the same optics for excitation and detection and same modulation frequency).

To demonstrate pH sensing using cells and FLIM instrumentation we have loaded yeast cells with pH probe Oregon Green 488. This probe is available in cell permeable form from Molecular Probes. It was found that Oregon Green displays sufficient lifetime pH response, is well loaded

into cells and also provides ability for extra-cellular pH sensing as well. Figure 9 shows a cell image and calibration curves using Oregon Green 488 probe.

Our work on oxygen and pH intra- and extra-cellular imaging has been presented at NASA 2003 Cell Science Conference [12].
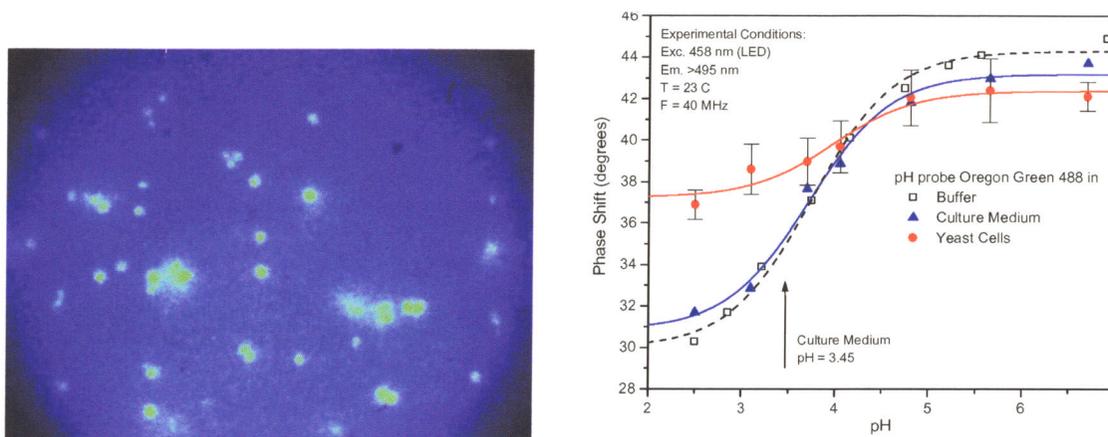
Figure 9. pH Left: Intensity image of PH probe Oregon Green 488 loaded into a yeast cells (green small areas) and in culture medium (blue intermediate area). Right: pH measurement using FLIM instrumentation shows that Oregon Green displays a pH response in culture medium similar to the externally buffered solution.

1.3 Glucose probes evaluation

Two glucose probes that display lifetime sensitivity to glucose have been identified and tested for cell culture applications. These probes have been synthesized at the University of Maryland at Baltimore. These are 9-[[N-Methyl-N-(o-boronobenzyl)amino]methyl]anthracene **(Probe 1)** and 9-10-bis [[N-Methyl-N-(o-boronobenzyl)amino]methyl]anthracene **(Probe 2).** They were previously characterized in solutions with high content of methanol. For NASA applications related to cellular research an environment with high content of alcohol is not desired; it will affect cell growth and cellular metabolism. Therefore, we have evaluated glucose sensitivity of both probes with decreased methanol content. Probe 2 has higher glucose sensitivity in terms of larger changes of its spectral properties and detection of smaller glucose concentration. However, we observed substantial reduction of Probe 2's sensitivity in decreased methanol content that may preclude its use for culture media. More work would be needed to determine the experimental conditions for practical use of Probe 2.

Probe 1 is less sensitive to glucose; both in spectral changes and in glucose concentrations as reported by University of Maryland. However, our data obtained for Probe 1 was very promising. In contrast to Probe 2, Probe 1 displays sufficient glucose sensitivity in the PBS buffer in very low methanol content (stock solution in Methanol). Figure 10 shows the glucose-dependent phase angles in the presence of 33% and 0.4 % of methanol. Three culture media with various chemical compositions were tested using Probe 1. It was found that Dulbecco's Modified Eagle Medium (High glucose content) and Grace's Insect Medium (high concentration of lactalbumin and yeastolate saturates Probe 1. It was also observed that Probe 1 displayed glucose response in the SF-900 II SFM medium.

Our investigations of glucose probes indicate that straightforward use of probes in culture media may cause problems in terms of sensitivity and unexpected interactions of probe molecules with biomolecules in the media. It is recommended to encapsulate probes in glucose permeable membranes to avoid interference.

10
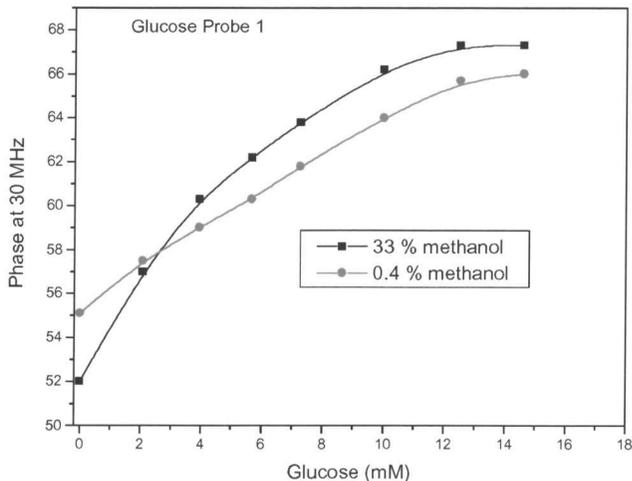
Figure 10. Glucose Probe 1 shows good glucose sensitivity in the presence of small amount of methanl in aqueous solution. Experiment was carried out at room temperature with two levels of methanol in buffered solution: 33 an 0.4 %. Excitation was 375 nm using UV LED and observation above 410 nm.

2.   Support the Delivery of the Space Qualified System (Task 4)

Under this contract FLIM instrumentation and software has been developed and tested. The FLIM software, written in VB.NET, uses an advanced, fault-tolerant state machine architecture to drive the capture hardware (modulation module for image intensifier and CCD camera) and the capture GUI. An integrated VB.NET analysis package extracts phase, modulation, and intensity images, using a linear curve fitting procedure to compute the FLIM coefficients. Various additional analysis tools (background subtraction, masking, binning, etc.) are also integrated into the suite, and can be automated for ease of use. The algorithms have been validated by comparing their output, at selected pixels in a variety of image series, to independently computed FLIM coefficients (average areas) derived from Origin, a third party analysis software package, and to various known samples, as described in our monthly reports.

Sensors and probes for oxygen and pH have been developed and we have shown their application for intra-and extra-cellular measurements. Documentation of all of our work under this contract, in the form of monthly and annual reports, tables, graphs and publications, has been provided.

The property acquired for contract effort will be shipped to the Marshall Space Flight Center before August 30, 2003. This property includes:
1. Cell culture Incubator (NAPCO)
2. Freezer (-85C) (Revco)
3. Refrigerator (VWR)
4. Frequency-Domain Fluorometer (ISS, Inc.)
5. Rotovapor
6. Balance (Ohaus Corporation)

References

1. Szmacinski H. and Chang Q. Micro- and Sun-nanosecond Lifetime Measurements Using a UV Light Emitting Diode. Applied Spectrosc. 54:106-109, 2000.
2. Richmond, R., Chang, T.Y., Lu, X., and Malak, H. Distribution and Spectroscopy of reen Fluorescent Protein and Acyl-CoA:Cholesterol Acyltransferase in Sf21 Insect Cells. Presented at the 2-nd Pan-Pacific Basin Workshop on Microgravity Sciences, Pasadena, alifornia, May 2001.
3. Lakowicz, J.R, Szmacinski, H. and Johnson, M.L. Fluorescence lifetime imaging microscopy: homodyne technique using high-speed gated image intensifier. Methods Enzymol., 240, 723, 1994.
4. Schneider, P.C. and Clegg, R.M. Rapid acquisition, analysis, and display of fluorescence lifetime-resolved images for real applications. Rev. Sci. Instrum., 68, 4107, 1997.
5. Pugh V., Malak H., Szmacinski H., and Moore W.E. Novel Luminescent Ru(II) Metal-Ligand Oxygen Probes for Two-Photon Excitation Fluorescence Microscopy. J. Fluorescence 2003, submitted.
6. Castellano, P. and Lakowicz J.R. A Water-Soluble Luminescence Oxygen Sensor. Photochem. Photobiol. 67(2):179, 1998.
7. Murtaza M, Chang Q, Rao G., Lin H., Lakowicz, J.R. Analytical Biochemistry 247:216, 1997.
8. Pugh V. A Novel pH sensitive dye and use in pH sensind device, US Patent application 60/400,661.
9. Szmacinski H., Lakowicz J.R. Optical Measurements of pH Using Fluorescence Lifetimes and Phase-Modulation Fluorometry. Anal. Chem. 65: 1666-1674, 1993.
10. Lin, H-J., Szmacinski H., Lakowicz J.R. Lifetime-Based pH Sensors: Indicators for Acidic Environments. Anal. Biochem. 269:162-167, 1999.
11. Lin, H-J., Herman P., Kang J-S., Lakowicz J.R. Fluorescence lifetime characterization of novel low pH probes. Anal. Biochem. 294:118-125, 2001.
12. Szmacinski H., and Pugh V. Optical Micro-Sensors for Cellular Studies of Oxygen and Nutrients. Presentation at the 2003 NASA Cell Science Conference, February 20-22, 2003, Huston, Texas.

Dr. Henryk Szmacinski
PI of NASA contract

REPORT DOCUMENTATION PAGE

Form Approved
OMB No. 0704-0188

The public reporting burden for this collection of information is estimated to average 1 hour per response, including the time for reviewing instructions, searching existing data sources, gathering and maintaining the data needed, and completing and reviewing the collection of information. Send comments regarding this burden estimate or any other aspect of this collection of information, including suggestions for reducing this burden, to Department of Defense, Washington Headquarters Services, Directorate for Information Operations and Reports (0704-0188), 1215 Jefferson Davis Highway, Suite 1204, Arlington, VA 22202-4302. Respondents should be aware that notwithstanding any other provision of law, no person shall be subject to any penalty for failing to comply with a collection of information if it does not display a currently valid OMB control number.
PLEASE DO NOT RETURN YOUR FORM TO THE ABOVE ADDRESS.

1. REPORT DATE (DD-MM-YYYY)	2. REPORT TYPE	3. DATES COVERED (From - To)
15-08-2003	Final	May 1999 - July 2003

4. TITLE AND SUBTITLE

Cellular Oxygen and Nutrient Sensing in Microgravity Using Time Resolved Fluorescence Microscopy

5a. CONTRACT NUMBER

NAS8-99070

5b. GRANT NUMBER

5c. PROGRAM ELEMENT NUMBER

6. AUTHOR(S)

Szmacinski, Henryk, Ph.D.

5d. PROJECT NUMBER

5e. TASK NUMBER

5f. WORK UNIT NUMBER

7. PERFORMING ORGANIZATION NAME(S) AND ADDRESS(ES)

Microcosm, Inc.
9140 Guilford Road, Suite O
Columbia, MD 21046

8. PERFORMING ORGANIZATION REPORT NUMBER

Final

9. SPONSORING/MONITORING AGENCY NAME(S) AND ADDRESS(ES)

National Aeronautics and Space Administration
George C. Marshall Space Flight Center
Marshall Space Flight Center, AL 35812

10. SPONSORING/MONITOR'S ACRONYM(S)

NASA, MSFC

11. SPONSORING/MONITORING REPORT NUMBER

12. DISTRIBUTION/AVAILABILITY STATEMENT

Unlimited Unclassified

13. SUPPLEMENTARY NOTES

14. ABSTRACT

Oxygen and nutrient sensing is fundamental to the understanding of cell growth and metabolism. This requires identification of optical probes and suitable detection technology without complex calibration procedures. Under this project Microcosm developed an experimental technique that allows for simultaneous imaging of intra- and inter-cellular events. The technique consists of frequency-domain Fluorescence Lifetetime Imaging Microscopy (FLIM), a set of identified oxygen and pH probes, and methods for fabrication of microsensors. Specifications for electronic and optical components of FLIM instrumentation are provided. Hardware and software were developed for data acquisition and anlysis.. Principles, procedures, and representative images are demonstrated. Suitable lifetime sensitive oxygen, pH, and glucose probes for intra- and extra-cellular measurements of analyte concentrations have been identified and tested. Lifetime sensing and imaging have been performed using PBS buffer, culture media, and yeast cells as a model systems. Spectral specifications, calibration curves, and probes availability are also provided in the report.

15. SUBJECT TERMS

oxygen sensing, pH sensing, time-resolved fluorescence, fluoescence microscopy, optical imaging

16. SECURITY CLASSIFICATION OF:			17. LIMITATION OF ABSTRACT	18. NUMBER OF PAGES	19b. NAME OF RESPONSIBLE PERSON
a. REPORT	b. ABSTRACT	c. THIS PAGE			Henryk Szmacinski
Unclassified	Unclassified	Unclassified	UU	1	19b. TELEPHONE NUMBER (Include area code) (301) 725-2775

Standard Form 298 (Rev. 8-98)
Prescribed by ANSI Std. Z39-18